SSRG International Journal of Civil Engineering
ISSN: 2348-8352/ https://doi.org/10.14445/23488352/IJCE-V12I11P121

Volume 12 Issue 11, 276-292, November 2025
© 2025 Seventh Sense Research Group®

Original Article

Studies on Durability and Carbonation Characteristics of Limestone Calcined Caly Cement by Varying Clinker and GGBS Content

K. Venkataraman[1], P.R. Kannan Rajkumar[2]

[1,2]*Department of Civil Engineering, Faculty of Engineering and Technology, SRM Institute of Science and Technology, Kattankulathur, Tamil Nadu, India.*

[1]*Corresponding Author : kannanrp@srmist.edu.in*

Received: 12 September 2025 Revised: 14 October 2025 Accepted: 11 November 2025 Published: 29 November 2025

Abstract *- Ordinary Portland Cement (OPC) production leads to CO_2 emission, representing around 5%-10% of total emissions globally. To minimize these emissions, the Supplementary Cementitious Materials (SCMs) are being used as a partial replacement for Portland clinker, including LC3 cement. Studies on the durability properties of LC3 concrete comprising SCMs as a binary blended mix are limited. Hence, this study aimed to examine the durability and carbonation behavior of LC3 concrete with partial replacement (10%) of GGBS. It was found that the loss in weight and strength of the 10% GGBS-added LC3 concrete was slightly higher compared to conventional LC3 concrete mix after exposure to acid, sulphate, and chloride attack, because of the slower hydration kinetics of GGBS. The incorporation of 10% GGBS into LC3 concrete increases the carbonation depth by 6.67%, 16.67% and 17.24% at 120 days for M25-LC3, M30-LC3, and M50-LC3 concrete mix, respectively. The high compressive strength concrete possesses superior durability properties compared to the low compressive strength concrete, with lower strength loss, weight loss, reduced chloride penetration, and better carbonation resistance due to its dense microstructure. It was concluded that the inclusion of GGBS introduces a trade-off between sustainability and early-age resistance to chloride and carbonation due to delayed pozzolanic activity.*

Keywords *- Global warming, Supplementary Cementitious Materials, Sustainability, Pozzolanic reaction, Porosity.*

1. Introduction

It has been mentioned that the cement industry contributes approximately 12%-15% to the total energy consumed in the global industrial sector [1, 2], with the cost of energy used being around 20%-40% of the total production costs [3]. Cement production is another major contributor of carbon dioxide emissions, representing approximately 8% of total CO_2 emissions [4]. Therefore, several approaches have been suggested, such as the development of low-carbon cement and the optimization of the cement clinker production process to control carbon emissions and their effects on climate change [5]. Among different approaches, one of the simplest and most efficient approaches to decrease the carbon footprint of cement production is to use industrial waste as a partial alternative for cement. However, the supply of conventional SCMs, such as GGBS, silica fume, and fly ash, remains limited in relation to the demand for cement [6]. Conversely, Kaolinite clays are abundantly found in Earth's crust and could be utilized as a replacement for cement by thermal activation [7]. This results in dihydroxylation of kaolinite into metakaolin [8], a pozzolanic substance that reacts with portlandite produced cement hydration and water to generate C-A-S-H [9]. Most kaolinite clay deposits are impure and comprise other phases that are considered impurities, like iron, quartz, calcite, titanium oxides, and several other types of clay [10]. A recent study has demonstrated that incorporating low or medium purity of calcined clay (i.e., kaolinite) leads to excellent concrete properties [11]. Clays need to be calcined before being utilized in concrete to produce highly reactive amorphous metakaolin through the dihydroxylation of crystalline kaolinite. The optimum calcination temperature for the kaolinite clay ranges between 750℃ and 850 ℃ [12]. A recent study on using Kaolinitic clay as SCM in concrete has gained interest in recent years. The first and second "International Conference on calcined clay for sustainable concrete" [13-15] brought numerous research efforts in progress. It was reported that utilization of Kaolinitic clay above 30% replacement level might result in a decline in mechanical properties [16]. To increase the replacement level of kaolinite clay without compromising the mechanical properties, the limestone (CaCO3) was mixed with Portland cement clinker and calcined clay. It reacts with C3A in the clinker and portlandite to form monocarboaluminate phase [17]. The aluminates derived from metakaolin react with limestone, promoting the formation of carboaluminate phases. This three-component system, which consists of calcined clay, limestone, and Portland clinker, is referred to as Limestone Calcined Clay Cement (LC3) [18]. Several authors have investigated the mechanical behavior of LC3 concrete [8, 11, 19-22]. Durability is the primary concern for the concrete structure, especially the steel bar corrosion caused by penetration of chloride ions, which can come from sources like seawater or deicing salts. The transport rate of iron in concrete is primarily affected by its physical pores and the physical and chemical reactions of chloride ions with hydrates, in particular the C-A-S-H and AFm phases. In general, the utilization of SCMs in concrete increases its resistance to ion transport, primarily due to the improvement of porosity. It was reported that with a 50% replacement level of OPC by kaolinite clay with the addition of limestone, LC3 exhibits enhanced durability in terms of chloride resistance and the Alkali-Silica Reaction (ASR) [22]. Dhandapani et al. (2018) [19] found that the LC3 concrete possesses higher resistivity than the fly ash and OPC concrete. They also observed that the fly ash concrete mix increases durability after 90 days, while LC3 exhibits much better durability performance within 28 days without the need for extended curing. Shiva Kumar et al. (2023) explored the use of LC3 as a partial replacement for cement clinker at a 50% replacement level in concrete and found that the durability of the LC3 concrete was better compared to PPC and OPC concrete [23]. Ram et al. (2022) found that the kaolinite content possesses a moderate impact on compressive strength of concrete and a significant impact on the durability properties of concrete [24]. They observed that using kaolinite content of 40% decreases the chloride migration by 50% and diffusion coefficient by 36% in comparison to OPC concrete. Dhandapani et al. (2018) found that LC3 concrete has an increased autogenous shrinkage and comparable total shrinkage in comparison to OPC concrete [19]. Scrivener et al. (2018b) showed that LC3 paste demonstrated the same level of autogenous shrinkage as the OPC paste in the case of 28 days of curing [25]. Nguyen et al. (2022) observed that LC3 concrete exhibits higher autogenous shrinkage in ages of up to 100 days, because of a more refined pore structure [26]. Abdulqader et al. (2023) discovered that the LC3 mix showed noticeably less drying shrinkage as compared to OPC [27]. Many studies have explored the carbonation of LC3 concrete and provided valuable insight, including the carbonation depth, duration, etc [28-31]. Scrivener et al. (2018a) discovered that the carbonation depth of LC3 concrete was higher compared to OPC and OPC calcined clay mix after 2 years of natural carbonation [7]. Khan et al. (2018) demonstrated that carbonation penetration steadily rises as the replacement level of OPC increases [32]. Shah et al. (2018) explored the carbonation depth of the LC3 concrete, thereby comparing it with fly ash and OPC concrete under both natural and accelerated environments [33]. It was reported that the significant challenges for the on-site application of LC3 were its relatively low resistance to carbonation [34].

Research on the LC3 concrete system has progressed significantly; however, key gaps remain, especially in investigating the interactions of various SCMs such as silica fume, fly ash, GGBS, nano silica, etc., into the mix that include kaolinite clay and the limestone [35, 36]. Indeed, limited research has been available on investigating the interactions of various SCMs, such as silica fume, fly ash, GGBS, nano silica, etc., into the concrete mix that includes kaolinite clay and limestone in terms of its mechanical properties. However, their durability properties are not highly reported in the existing studies. At this point, it is essential to assess the durability properties, since improved durability lowers maintenance costs and the need for virgin raw materials. In this regard, concrete carbonation is a significant factor for evaluating the service life and durability of reinforced concrete structures concerning the risk of corrosion in the reinforcement. LC3 systems inherently have a high-water demand because of the inclusion of calcined clay [37].

As water is a scarce natural resource, addressing the problem of water demand is essential to improve the sustainability of cement [36]. Therefore, LC3 cement often rEquationires an overdosage of superplasticizers, which considerably raises the carbon footprint of the cement [27, 37]. Hence, it is crucial to determine a specific approach aimed at addressing the challenge of LC3. In contrast, GGBS, with its smoother texture and smaller particle size, might enhance the workability and decrease water demand. Mixing calcined clay with GGBS can improve particle packing density, thereby minimizing water demands and improving the properties of LC3 concrete. Therefore, this study attempts to explore the effect of the inclusion of GGBS content on LC3 concrete in terms of durability and carbonation properties.

2. Research Significance

This study investigates sustainable concrete solutions by optimizing LC3 with 10% GGBS, addressing durability, carbonation, and sustainability challenges for M25, M30, and M50 grades of concrete, thereby ensuring practical application. While numerous studies have concentrated on LC3 cement as a binary substitute for OPC, there is a dearth of studies on the durability properties of LC3 concrete containing SCMs. Understanding the synergistic impacts of these SCMs with LC3 is vital for enhancing concrete performance, especially concerning durability, sustainability, and cost-effectiveness. This is crucial for real-world applications in infrastructure where long-lasting durability, lower carbon footprint, and improved material performance are critical. The addition of GGBS improves workability, decreases water demand, and lessens the need for superplasticiser, thereby enhancing durability and reducing costs. By using industrial by-products such as GGBS, this study promotes resource efficiency, decreases CO2 emissions, and prolongs service life, providing valuable insights on sustainable, high-performance concrete for resilient and environmentally friendly infrastructure projects.

3. Materials and Methodology

The primary aim of this study is to examine the impact of substituting 10% GGBS in LC3 concrete regarding its durability properties. The various durability properties of the LC3 concrete, as well as the LC3+10% GGBS concrete mix for M25, M30, and M50 grades, were compared to gain insights into the impact of GGBS on the durability properties of the LC3 concrete.

3.1. Materials

3.1.1. Limestone Calcined Clay Cement (LC3)

The innovative cement, called LC3, consists of 40% Portland clinker, 40% calcined clay, and 20% limestone, which is used as a primary binder for the concrete. Tables 1 and 2 outline the physical properties and chemical composition of the LC3 cement.

Table 1. Physical properties of LC3

Properties	Fineness (m^2/mg)	Normal consistency (%)	Setting time (min)		Compressive strength (MPa)		
			Initial	Final	3-days	7-days	14-days
Values	386	32.5	30	105	34.3	45.3	50.6

Table 2. Chemical composition of LC3

Composition	CaO	SiO_2	Fe_2O_3	Al_2O_3	SO_3	MgO	Na_2O	K_2O	Chloride	LOI
%	30.35	34.28	3.43	19.45	1.58	1.38	0.31	0.27	0.027	8.21

Table 3. Chemical composition of GGBS

Elements	SiO_2	CaO	Al_2O_3	Fe_2O_3	MgO	Na_2O	K_2O	LOI
%	21.58	55.25	14.88	1.78	2.63	0.015	0.48	1.8

Figure 1 illustrates the X-ray Diffraction (XRD) of the GGBS captured with Cu-K (1.5418 A°) radiation over a 2-hour period, utilizing a Bruker D2 phase X-ray diffractometer. The XRD pattern of LC3 cement highlights its mineral phase with dominant peaks for Quartz (Q), Calcite (C), and Mullite (M), indicating the contributions of calcine clay and limestone. The presence of residual Kaolinite (K) and Illite (I) signifies incomplete dehydroxylation and the possibility for optimizing the calcination process.

Minor phases such as Anatase (A), Rutile (R), and Hematite (H) suggest the presence of titanium and iron-rich compounds contributing to hydration properties and colour of the cement. The synergy between reactive alumino-silicates, such as mullite, and limestone enhances the pozzolanic activity, strength, and durability of cement composites, whereas the residual kaolinite provides a gradual hydration [10].

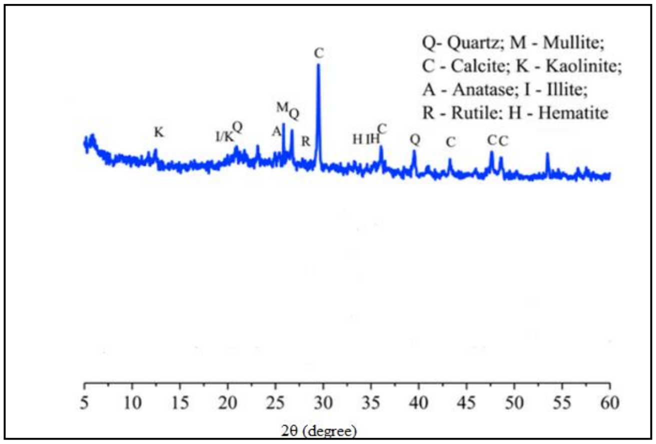

Fig. 1 XRD of LC3

3.1.2. GGBS

GGBS, an industrial by-product from the steel manufacturing industry, was utilized as a secondary binding material for the concrete in this study. The limestone, coke, and iron ore are heated in the kiln at a temperature of about 1500℃ – 1600℃. It generally includes aluminous and grainy siliceous deposits. The GGBS was used as SCMs to the LC3 at a replacement level of 10%. Tables 3 and 4 define the chemical composition and properties of GGBS.

The XRD analysis of GGBS was carried out using a Bruker D2 diffractometer with Cu-Kα radiation ($\lambda = 1.5418$ Å), scanning over a 2θ range of 10° to 80° with a step interval of 0.02°/1s. As shown in Figure 2, the diffraction peaks observed between 10°–20° and 28°–31° indicate the presence of a significant amount of amorphous calcite in the GGBS sample.

Table 4. Properties of GGBS

Properties	Value
Color	White
Finess (m^2/kg)	382
Specific gravity	2.82
Bulk density (kg/m^3)	1200

3.1.3. Fine Aggregates

M-sand that complies with zone-II of the IS: 383-1970 standard was utilized as a fine aggregate for concrete sample preparation [38]. Its various properties, including specific gravity and fineness modulus, were tested in accordance with the IS: 2386 (Part 1)-1963 and found to be 2.6 and 2.7 (IS:2386 (Part III)-1963 n.d.) [39].

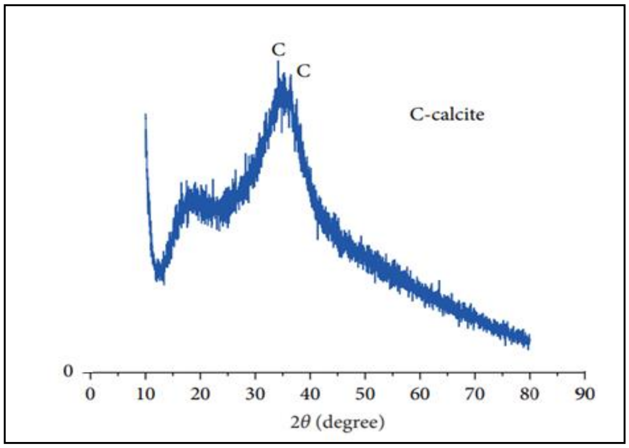

Fig. 2 XRD of GGBS

3.1.4. Coarse Aggregates

The granite, which is well-graded and has an angular shape with a maximum particle size of 12.5 mm, was employed as a coarse aggregate for concrete as per IS: 383-1970 standard. Its various properties, including specific gravity, water absorption, and fineness modulus, were evaluated according to IS: 2386 (Part 1)-1963 and IS: 2386 (Part 3)-1963, and found to be 2.7, 7.2, and 0.62% (IS:2386 (Part III)-1963 n.d.) [39].

3.1.5. Super Plasticizer

A high-range water-reducing admixture, such as a superplasticiser whose specific gravity is 1.82 with 25% solid content, was employed as a concrete admixture. The concentration of superplasticizer used in the concrete mix was in the 0.75% to 1% by weight of cement, irrespective of the weight of cement.

3.2. Mix Proportioning

The mix ratio for the M25, M30, and M50 grade concrete was proportioned according to IS: 10262-2019 to achieve their respective target strength (IS-10262:2019 n.d.)[40]. After various trial mixes with various replacement level of GGBS into the LC3 concrete mix, optimized properties such as slump and compressive strength were achieved with a 10% replacement level of GGBS. Hence, 10% of GGBS was used as an optimum replacement level for the preparation of concrete samples. Initially, M-sand and coarse aggregate were added into the concrete mixer and thoroughly mixed for a period of 2 minutes in dry conditions. Then, the water-superplasticizer mixture was added to it and continued mixing for around 4 minutes. The fresh concrete mix was filled into a cube, cylinder, and prism mould to make test specimens as per IS: 516-2021 and IS: 5816-1959 and allowed to cure for 28 days (IS 516 (Part 1/Sec 1) : 2021 n.d.) [41].

Table 5. Mix proportioning

Materials	M25-LC3	M25-LC3+10% GGBS	M30-LC3	M30-LC3+10%GGBS	M50-LC3	M50-LC3+10% GGBS
Cement (kg/m^3)	310	279	322	290	340	306
GGBS (kg/m^3)	-	31	-	32	-	34
M-Sand (kg/m^3)	790	780	783	761	832	832
Coarse Aggregate (kg/m^3)	1220	1215	1209	1204	1120	1120
W/C	0.55	0.55	0.55	0.55	0.46	0.46
Super Plasticizer	0.9%	0.8%	1.0%	0.8%	0.85%	0.75%

3.3. Experimental Investigation

The primary aim of this study is to examine the effect of the inclusion of GGBS at a 10% replacement level for LC3 cement on the durability properties of the concrete. Accordingly, various tests like acid attack, chloride attack, sulphate attack, RCPT, water permeability test, drying shrinkage, and carbonation have been planned and conducted as per IS standards, respectively.

3.3.1. Durability Studies

Acid Attack

This study employed the acid attack test to assess the acid resistance capacity of LC3-M30, LC3-M30+10% GGBS, LC3-M50, and LC3-M50+10% GGBS concrete specimens. According to ASTM C267 standards, the weight and strength loss were determined after exposing a 100mm concrete cube specimen to a 3% concentration of H_2SO_4 solution maintained at 27± 2°C (ASTM C267, 2001) [42]. After 30-days, 60-days, 90-days, 120-days, 150-days, and 180-days of immersion of the cube specimen in the acid solution, the specimens were taken out, surface cleaned, and then weighed to assess the loss in weight. Also, the specimen was subjected to compression testing using a UTM to assess the strength loss.

Sulphate Attack

According to ASTM C267 standards, the sulphate attack test is used to measure the sulphate resistance capacity of LC3-M30, LC3-M30+10% GGBS, LC3-M50, and LC3-M50+10%

GGBS concrete specimens by measuring the weight loss and strength loss after exposure to sulphate solutions (ASTM C267, 2001). The sulphate resistance capacity of the LC3-M30, LC3-M30+10% GGBS, LC3-M50, and LC3-M50+10% GGBS concrete was assessed by measuring the weight and strength loss after exposing 100mm concrete cube specimens to acid solutions of 5% concentration of $MgSO_4$ solution maintained at 27±2℃. After 30-days, 60-days, 90-days, 120-days, 150-days, and 180-days of immersion of the cube specimen in the sulphate solution, the specimens were taken out, surface cleaned, and then weighed to assess the loss in weight. Also, the specimen was subjected to compression testing using a UTM to assess the strength loss.

Chloride Attack

The chloride attack was used to determine the chloride resistance capacity of the LC3-M30, LC3-M30+10% GGBS, LC3-M50, and LC3-M50+10% GGBS concrete specimens. According to ASTM C267 standards, the weight loss and strength loss were measured after exposing the 100mm concrete cube specimen to 5% concentration of NaCl solution maintained at 27±2℃ ASTM C267, 2001). After 30-days, 60-days, 90-days, 120-days, 150-days, and 180-days of immersion of the cube specimen in the sulphate solution, the specimens were taken out from the NaCl solution, surface cleaned, and then weighed to assess the loss in weight. Also, the specimen was subjected to compression testing using a UTM to assess the strength loss.

Water Absorption Test

The cube specimen of size 100mm was used to measure the water absorption capacity of the LC3-M30, LC3-M30+10% GGBS, LC3-M50, and LC3-M50+10% GGBS concrete specimens as per ASTM C 642-13 guidelines (ASTM C642-97 1997) [43]. After 28 days of curing, the specimen was oven-dried at 105 ± 5℃. The specimen was cooled at room temperature and weighed (W1). Then, the specimen was immersed in the water tank for 24 hours. After 24 hours of being submerged in the water tank, the specimen was removed from the water tank, and its weight (W2) was measured. The water absorption capacity of the specimen was measured using the Equationation. (1);

$$Water\ Absorption\ (\%) = \frac{(W_2-W_1)}{W_1}\ x\ 100 \tag{1}$$

Where W_2 indicates saturated weight of cube (kg); W_1 is the dried weight of the cube (kg).

Rapid Chloride Permeability Test (RCPT)

The durability of the RC structures typically depends upon their capacity to resist chloride ion penetration. Hence, it is essential to measure the chloride ion penetration capacity of the concrete. A cylindrical concrete specimen of the size 100mm x 200 mm was used to assess the chloride ion ingress resistance of the LC3-M30, LC3-M30+10% GGBS, LC3-M50, and LC3-M50+10% GGBS concrete specimens as per ASTM C1202 guidelines (ASTM C1202 2012). After 28-days and 90-days of curing, the cylindrical concrete specimens were sliced to a thickness of 50 mm and then kept in the RCPT apparatus and coated with epoxy resin. The test setup includes two containers filled with 0.3 M NaOH and 3% NaCl, charged with a 60 V DC for the ions. For a 6-hour period, the current was recorded at 30-minute intervals. Around 3 specimens were tested to determine the average RCPT value. The level of chloride ion penetration of the LC3 concrete samples was measured in terms of charge passed as compared with standard values as described in ASTM C1202.

3.3.2. Carbonation Studies

The carbonation depth of LC3-M30, LC3-M30+10% GGBS, LC3-M50, and LC3-M50+10% GGBS concrete specimens was determined as per IS 516 (Part 5/Sec 3): 2021 standards (IS 516 (Part 5/Sec 1) : 2021 n.d.). The prism specimens measuring were cast and encased in plastic for 24 hours at 27± 2 °C, after which they were removed and placed in an environmental condition with high humidity of about 95% for 28 days. A preconditioning of the sample is rEquationired for maintaining a relative humidity of 75 ± 2% and at a temperature of 27 ± 2 °C. Then, the specimen was positioned in the carbonation chamber at 5% CO_2 at a temperature of 27 ± 2 °C and a relative humidity of 75 ± 2%. To allow CO_2 diffusion between specimens, they were positioned with a minimum distance of 20 mm apart. The surfaces of the cut specimen were cleared of dust, and a phenolphthalein indicator was sprayed on the exposed surface. The portion of the concrete surface that exhibited a purple color was quickly measured and recorded within 10 minutes of spraying. A phenolphthalein indicator 1% ethanol solution was prepared using 1g of phenolphthalein and 90 ml of ethanol diluted to 100 ml of water. The carbonation depth values were measured as presented in Figure 3, which represents the average carbonation depth on each side as indicated by “e”, where $e = \frac{\sum(e_{1-4})}{4}$ The carbonation depth values measured show a maximum variation of about 20%. If the variation is more than 20%, both the values should be re-measured.

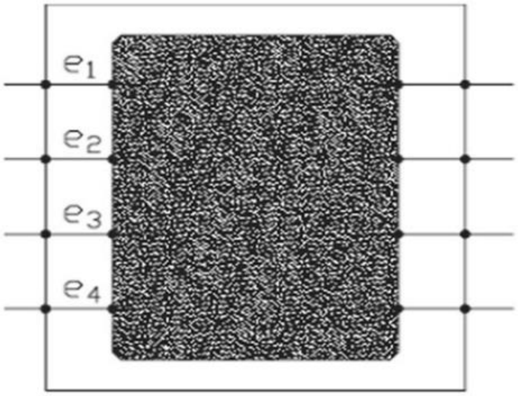

Fig. 3 Determination of carbonation depth

4. Results and Discussion

4.1. Acid Resistance of Concrete

4.1.1. Weight Loss

The weight loss (%) rate of various LC3 concrete specimens under acid solution attack was graphically presented in Figure 4. The weight loss of various LC3 concrete specimens consistently increases with an increase in exposure time, emphasizing the progressive interaction between the acid and concrete matrix. SO_4^{2-} react with free lime to produce gypsum as shown in Equation (2) [44]. Further, the gypsum reacts with C-A-H to develop ettringite as presented in Equation (3);

$$Ca(OH)_2 + H_2SO_4 \rightarrow CaSO_4.2H_2O \qquad (2)$$

$$3CaSO_4 + 3CaO.Al_2O_3.6H_2 + 25H_2 \rightarrow 3CaO.Al_2O_3.3CaSO_4.31H_2O \qquad (3)$$

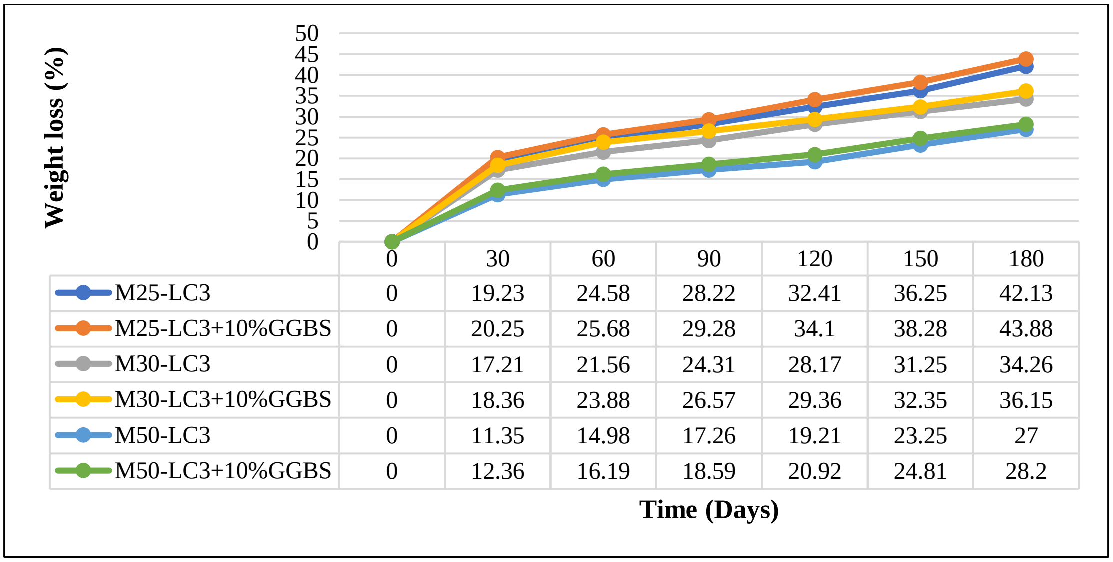

	0	30	60	90	120	150	180
M25-LC3	0	19.23	24.58	28.22	32.41	36.25	42.13
M25-LC3+10%GGBS	0	20.25	25.68	29.28	34.1	38.28	43.88
M30-LC3	0	17.21	21.56	24.31	28.17	31.25	34.26
M30-LC3+10%GGBS	0	18.36	23.88	26.57	29.36	32.35	36.15
M50-LC3	0	11.35	14.98	17.26	19.21	23.25	27
M50-LC3+10%GGBS	0	12.36	16.19	18.59	20.92	24.81	28.2

Fig. 4 Weight loss (%) of various LC3 concrete specimens after exposure to acid solution

The ettringite produced induces high internal stresses within the hydrated cement paste, leading to cracking, spalling, and loss in weight of the concrete [45, 46]. Higher compressive strength concrete, i.e., M50 grade concrete, is found to have higher acid resistance as compared to the low compressive strength concrete, such as M25 and M30 grade concrete, because of their low w/c, higher cement content, and dense matrix. For example, the weight loss of M25-LC3 concrete was 42.1%, whereas the weight loss of M50-LC3 concrete was only 27% at 180 days of acid attack. This same behavior is observed for all exposure times. Incorporating 10% of GGBS into the LC3 concrete mix slightly has a higher weight loss than the control LC3 concrete. For example, the weight loss of M25-LC3+10% GGBS concrete was 43.88%, whereas the weight loss of M25-LC3 concrete was 42.13% at 180 days of acid attack. This increased weight loss in GGBS added LC3 concrete might be due to reduced availability of $Ca(OH)_2$ for neutralizing the acid attack, as the hydration reaction of GGBS utilizes $Ca(OH)_2$ to develop additional C-S-H. These findings were found to be in line with Marangu (2021), [47], who also reported that the LC3 concrete mixes possess less weight loss.

4.1.2. Strength Loss

The strength loss (%) rate of various LC3 concrete specimens under acid solution attack was graphically presented in Figure 5. The sulfuric acid aggressively reacts with the $Ca(OH)_2$ in the hydrated cement paste as it produces expansive byproducts like gypsum and ettringite, which contribute to microstructural damage, increased porosity, and material loss [45, 46]. The findings reveal that strength loss progressively increased with increased exposure time for all concrete grades. This implies that with an increased exposure period, the filler behavior of the reaction products tends to dominate and occupies more volume than the products from which it is generated. This causes internal stresses and new crack formation, thus resulting in increased loss of compressive strength for all mixtures [48]. The strength loss of M25-LC3, M25-LC3+10%GGBS, M30-LC3, M30-LC3+10%GGBS, M50-LC3 and M50-LC3+10%GGBS concrete mixes at 30 days of acid exposure was 19.69%, 21.32%, 15.65%, 16.67%, 13.5% and 14.25% respectively; whereas it was increased to 41.86%, 4.01%, 38.24%, 40.23%, 35.29% and 37.69% at 180 days exposure. Further, it was found that the higher strength loss rate occurs in the initial exposure period, i.e., 0-90 days, than in the later stages, attributed to rapid ion exchange facilitated by a high concentration gradient initially, which slows over time due to pore clogging by degradation products. High compressive strength concrete, i.e., M50 grade concrete, was found to have less strength loss as compared to the low compressive strength concrete, such as M25 and M30 grade concrete, due to their low w/c ratio, higher cement content, and dense matrix. For example, at 180 days of exposure, the strength loss of M25-LC3 concrete was 41.86%, whereas the strength loss of the M50-LC3 concrete was only 35.29%. This superior performance of high-grade concrete, i.e., M50, can be attributed to its denser microstructure resulting from a lower w/c ratio of 0.46 and increased cement content, which limits the penetration of aggressive ions like SO_4^{2-} and H^+ ions. It was noted that adding 10% of GGBS into the LC3 slightly heightens the strength loss of LC3 concrete. For example, the strength loss of M25-LC3+10% GGBS concrete was 44.01%, whereas the weight loss of M25-LC3 concrete was marginally higher (41.86%) at 180 days of acid attack. Similarly, the strength loss of M50-LC3+10% GGBS concrete was 37.69%, whereas the weight loss of M50-LC3 concrete was marginally higher (35.29%) at 180 days of acid attacks. This behavior probably arises from GGBS consuming $Ca(OH)_2$ in a pozzolanic reaction to generate additional C-S-H, which limits the immediate neutralization of sulfuric acid. Thus, the decrease in buffering capacity facilitates the development of expansive byproducts like ettringite and gypsum, which heighten the degree of matrix deterioration.

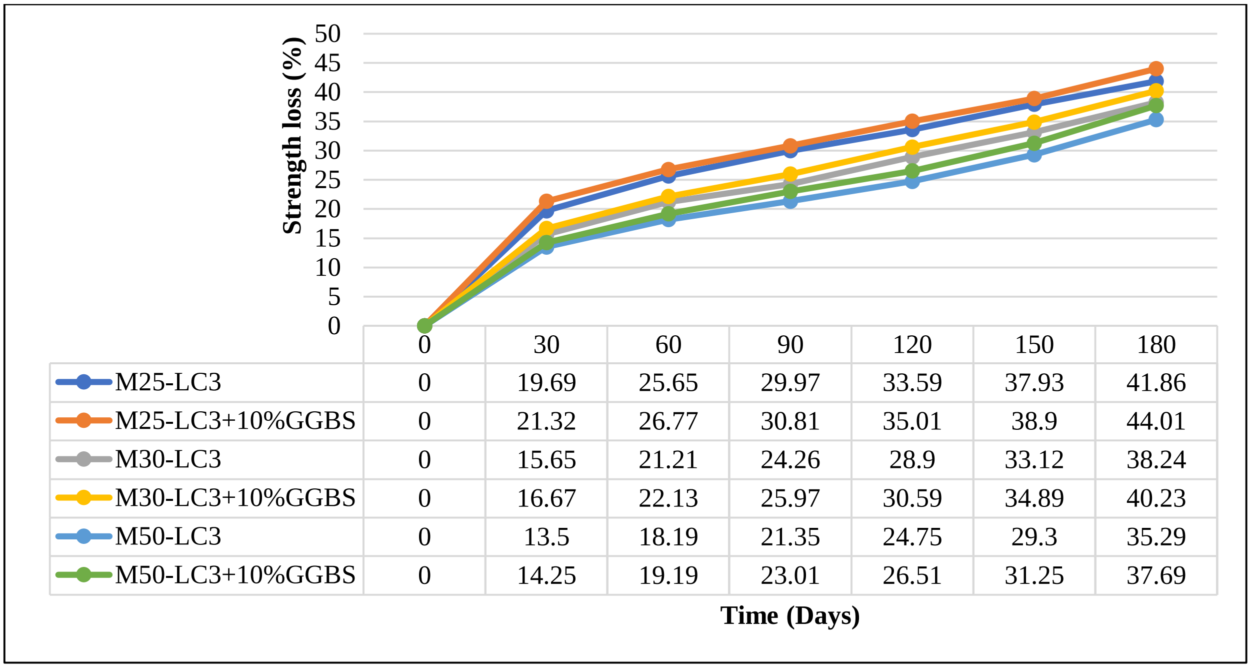

	0	30	60	90	120	150	180
M25-LC3	0	19.69	25.65	29.97	33.59	37.93	41.86
M25-LC3+10%GGBS	0	21.32	26.77	30.81	35.01	38.9	44.01
M30-LC3	0	15.65	21.21	24.26	28.9	33.12	38.24
M30-LC3+10%GGBS	0	16.67	22.13	25.97	30.59	34.89	40.23
M50-LC3	0	13.5	18.19	21.35	24.75	29.3	35.29
M50-LC3+10%GGBS	0	14.25	19.19	23.01	26.51	31.25	37.69

Fig. 5 Strength loss (%) of various LC3 concrete specimens after exposure to acid solution

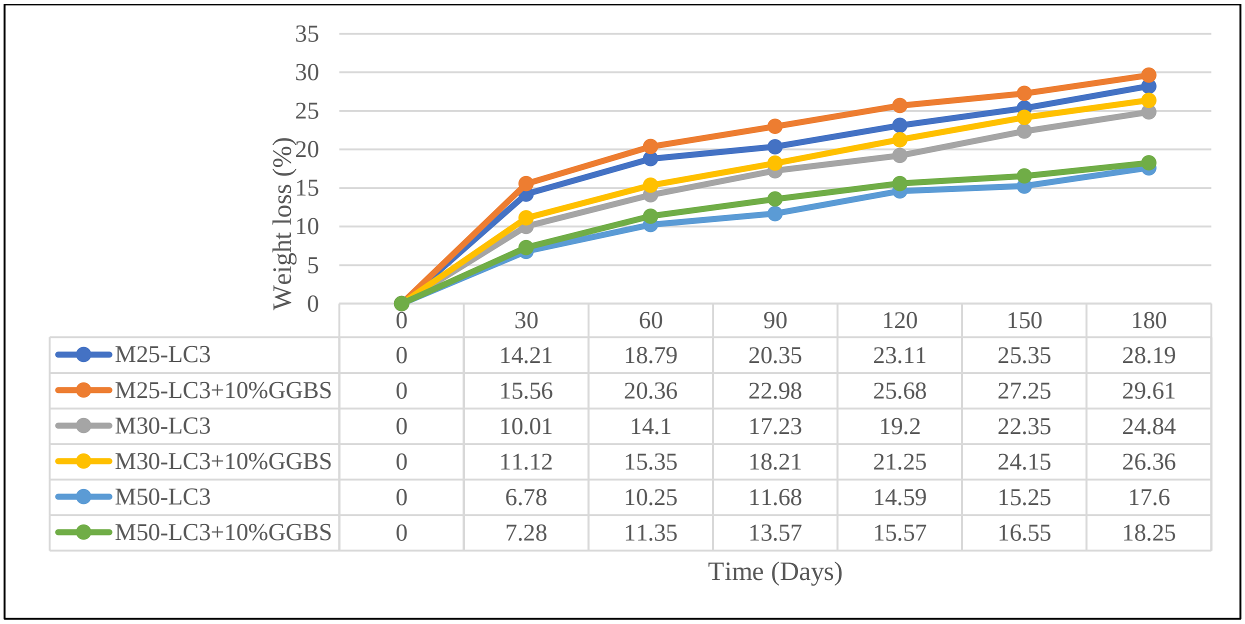

	0	30	60	90	120	150	180
M25-LC3	0	14.21	18.79	20.35	23.11	25.35	28.19
M25-LC3+10%GGBS	0	15.56	20.36	22.98	25.68	27.25	29.61
M30-LC3	0	10.01	14.1	17.23	19.2	22.35	24.84
M30-LC3+10%GGBS	0	11.12	15.35	18.21	21.25	24.15	26.36
M50-LC3	0	6.78	10.25	11.68	14.59	15.25	17.6
M50-LC3+10%GGBS	0	7.28	11.35	13.57	15.57	16.55	18.25

Fig. 6 Weight loss (%) of various LC3 concrete specimens after exposure to sulphate solution

4.2. Sulphate Attack

4.2.1. Mass Loss

The weight loss (%) rate of various LC3 concrete specimens under sulphate solution attack was graphically illustrated in Figure 6. The findings demonstrate that an increase in weight loss over time for all the concrete mixes, especially the higher weight loss, was observed for the low-grade concrete, i.e., M25 and M30. In particular, M25-LC3 lost 28.19% of its weight, while M50-LC3 lost only 17.6% of its weight during 180 days exposure period. The increased sulphate resistance observed in the M50 grade mix can be due to its denser microstructure, which arises from a lower water-cement ratio of 0.46. Denser mixes typically provide reduced permeability, thereby restricting the ingress of sulfate ions. The inclusion of 10% GGBS replacement presents slightly higher weight losses than the control LC3 concrete. For example, at 180 days, the M25-LC3+10% GGBS lost 29.61 % of its weight during 180 days exposure period, whereas M25-LC3 lost slightly less, about 28.19 % of its weight during 180 days exposure period. The interaction between LC3 and GGBS significantly affects sulfate resistance. LC3, composed of calcined clay and limestone, provides excellent chemical stability, while GGBS contributes a slowly reacting aluminosilicate component [49]. This delay in pozzolanic activity may lead to a less refined pore structure during the earlier curing days. A low replacement level, GGBS could compromise the synergistic sulfate-resisting properties of LC3 concrete, as it does not attain full reactivity within the observed period. The additional alumina from GGBS offers more sites for sulfate attack, which heightens the weight loss relative to the control LC3 mix.

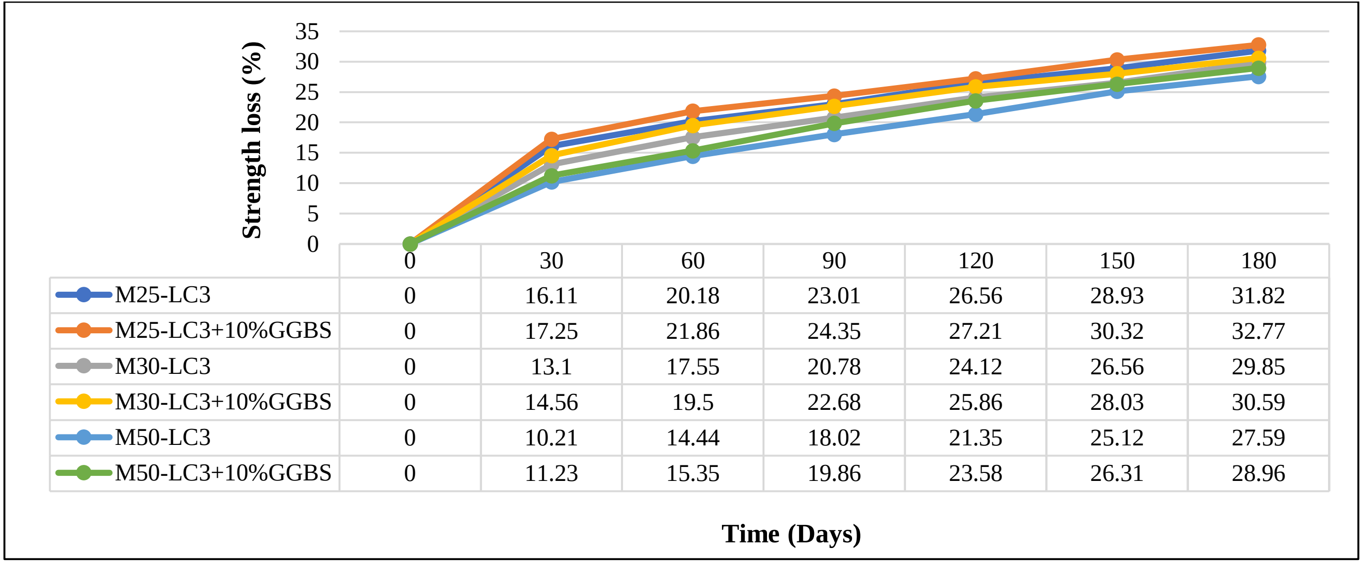

	0	30	60	90	120	150	180
M25-LC3	0	16.11	20.18	23.01	26.56	28.93	31.82
M25-LC3+10%GGBS	0	17.25	21.86	24.35	27.21	30.32	32.77
M30-LC3	0	13.1	17.55	20.78	24.12	26.56	29.85
M30-LC3+10%GGBS	0	14.56	19.5	22.68	25.86	28.03	30.59
M50-LC3	0	10.21	14.44	18.02	21.35	25.12	27.59
M50-LC3+10%GGBS	0	11.23	15.35	19.86	23.58	26.31	28.96

Fig. 7 Strength loss (%) of various LC3 concrete specimens after exposure to sulphate solution

4.2.2. Strength Loss

The strength loss (%) rate of various LC3 concrete specimens under sulphate solution attack was graphically presented in Figure 7. The results demonstrate a rise in strength loss over time. The interaction of hydrated cement with sulphate ions leads to variations in mass and strength, leading to the formation of secondary ettringite and changes in phase assemblage that may cause a strength loss [50]. Higher strength loss was observed for the low-grade concrete, i.e., M25 and M30. In particular, M25-LC3 lost 31.82% of its strength, while M50-LC3 lost only 27.59% of its strength during 180 days exposure period. The increased sulphate resistance observed in the M50 grade mix can be due to its denser microstructure, which arises from a lower water-cement ratio of 0.46. Denser mixes typically provide reduced permeability, thereby restricting the ingress of sulfate ions. The inclusion of 10% GGBS replacement presents slightly higher strength losses than the control LC3 concrete. For example, at 180 days, the M25-LC3+10% GGBS lost 32.77 % of its strength during 180 days exposure period, whereas M25-LC3 lost slightly less, about 31.82 % of its strength during 180 days exposure period. The comparatively reduced impact of sulphate attack on the LC3 concrete samples was due to refined pore structure and the reduction of tricalcium aluminate (C_3A) in the mix [50]. This results in an increasing consumption of $Ca(OH)_2$ because of the pozzolanic activity of the mineral additive. The higher strength loss with GGBS-added LC3 concrete may be due to the nature of the pozzolanic reaction, where GGBS forms additional C-S-H products, which may be initially susceptible to sulfate attack due to changes in pore structure and reduced availability of calcium hydroxide, $Ca(OH)_2$. Conversely, Lukowski & Salih (2015) reported that the strength loss of the GGBS-added OPC concrete was less than that of the OPC concrete [51]. In comparison, this study found that the strength loss of the GGBS-added LC3 concrete was higher than that of the conventional LC3 concrete. These contrasting results can be attributed to variations in hydration chemistry and interactions between materials. The inclusion of GGBS in OPC concrete mitigates the strength loss by reacting with $Ca(OH)_2$ formed during the hydration process to develop additional C-S-H gel. However, the calcined clay present in the LC3 cement consumes calcium hydroxide ($Ca(OH)_2$) through pozzolanic reactions, leaving minimal ($Ca(OH)_2$) for GGBS to react with, thus reducing its effectiveness. Moreover, the lower clinker content of LC3 and the distinct hydration dynamics of its constituents (limestone and calcined clay) might lead to less synergy with GGBS, causing a higher strength loss as compared to control LC3, when exposed to sulfate solution.

4.3. Chloride Attack

4.3.1. Mass Loss

The weight loss (%) rate of various LC3 concrete specimens under chloride solution attack was graphically presented in Figure 8. As the period of immersion of the concrete cube sample in NaCl prolongs, there is a tendency for increased weight loss as found in all concrete mixes. The pore structure resulting from the pozzolanic reaction might be slightly more interconnected initially, enabling higher ion ingress during prolonged exposure to aggressive solutions [52]. The high compressive strength concrete exhibits superior chloride resistance in terms of less weight loss as compared to the low compressive strength concrete mix. For example, the strength loss of M25-LC3 mix during 180 days exposure period was 19.62%, whereas the strength loss of M50-LC3 mix during 180 days exposure period was 15.36%. This demonstrates the superior chloride resistance of high-grade concrete as a result of its compact microstructure and the inherent advantages of reduced permeability, limiting the ingress of chloride ions. Additionally, the lower water-cement ratio minimizes capillary porosity [53]. However, higher weight loss was observed in M25 and M30 mixes because of their relatively porous structures, which facilitate deeper penetration of chloride ions, accelerating material degradation. It was noted that the incorporation of 10% GGBS in the LC3 Concrete contributes to increased strength loss across all concrete grades. The strength loss of M50-LC3 mix during 180 days exposure period was 15.36%, whereas the strength loss of M50-LC3+10%GGBS mix during 180 days exposure period was 16.79%. This same trend has been observed for both M30 and M25 grade concrete. In general, the inclusion of GGBS improves durability by reducing permeability and refining pore structures, although the depletion of free lime associated with GGBS replacement might lead to localized voids where chloride ion interacts with binding gels. This interaction accelerates microcracking and strength degradation over time [54].

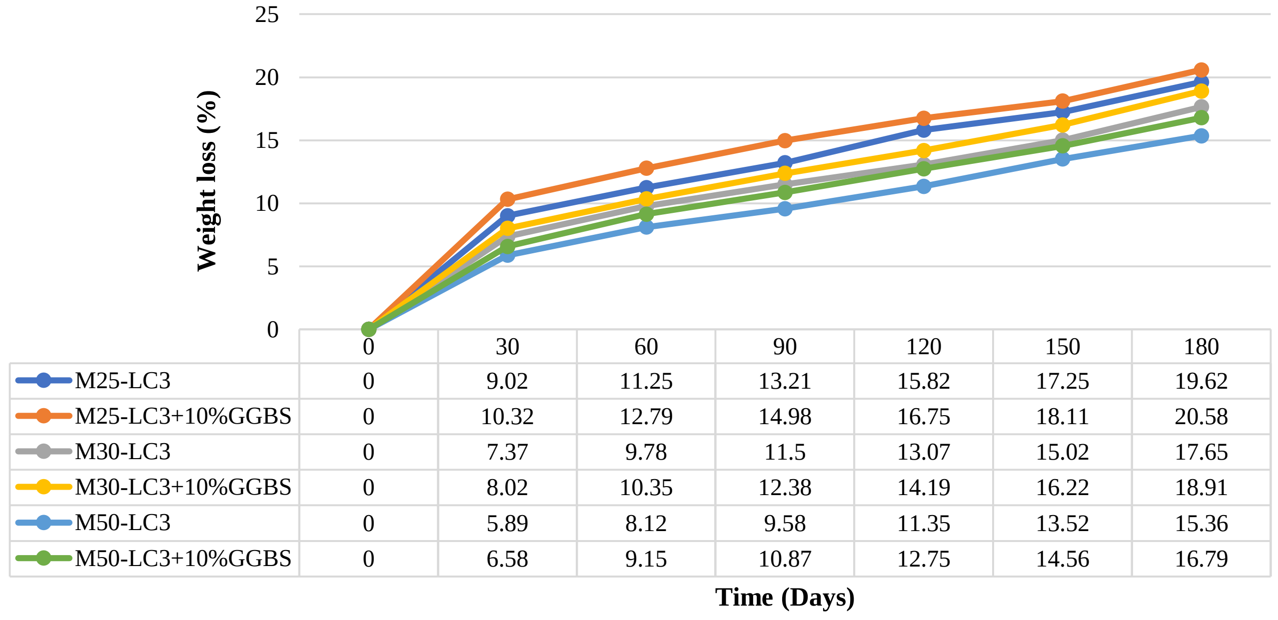

	0	30	60	90	120	150	180
M25-LC3	0	9.02	11.25	13.21	15.82	17.25	19.62
M25-LC3+10%GGBS	0	10.32	12.79	14.98	16.75	18.11	20.58
M30-LC3	0	7.37	9.78	11.5	13.07	15.02	17.65
M30-LC3+10%GGBS	0	8.02	10.35	12.38	14.19	16.22	18.91
M50-LC3	0	5.89	8.12	9.58	11.35	13.52	15.36
M50-LC3+10%GGBS	0	6.58	9.15	10.87	12.75	14.56	16.79

Fig. 8 Weight loss (%) of various LC3 concrete specimens after exposure to chloride solution

4.3.2. Strength Loss

The strength loss (%) rate of various LC3 concrete specimens under chloride solution attack was graphically presented in Figure 9. As the period of immersion of the concrete cube sample in NaCl prolongs, there is a tendency for increased strength loss as found in all concrete mixes. It was noted that a high compressive strength concrete mix exhibits superior chloride resistance in terms of less strength loss as compared to a low compressive strength concrete mix. For example, the strength loss of M25-LC3 mix during 180 days exposure period was 21.86%, whereas the strength loss of M50-LC3 mix during 180 days exposure period was 18.29%. This demonstrates the superior chloride resistance of high-grade concrete as a result of its dense microstructure. It was noted that using 10% GGBS in the LC3 concrete heightens the strength loss rate of all concrete grades. GGBS is recognized for its pozzolanic characteristics, which combine with $Ca(OH)_2$ generated during the hydration process to create additional C-S-H. Although this will improve long-term durability and reduce permeability, the partial replacement with GGBS changes the chemical condition of the concrete. When NaCl is present, chloride ions can infiltrate the concrete matrix and react with the hydration products. These reactions, especially the formation of Friedl's salts, rely on the availability of calcium aluminates as presented in Equation (4)

$$C_3A + CaCl_2 + 10H_2O \rightarrow C_3A.CaCl_2.10H_2O \tag{4}$$

The GGBS might decrease the quantity of C_3A in the system, potentially influencing the binding of chlorides and resulting in increased free chloride ion levels, accelerating the strength loss [54]. The strength loss of M50-LC3 mix during 180 days exposure period was 18.29%, whereas the strength loss of M50-LC3+10%GGBS mix during 180 days exposure period was 19.69%. This same trend has been observed for both M30 and M25 grade concrete.

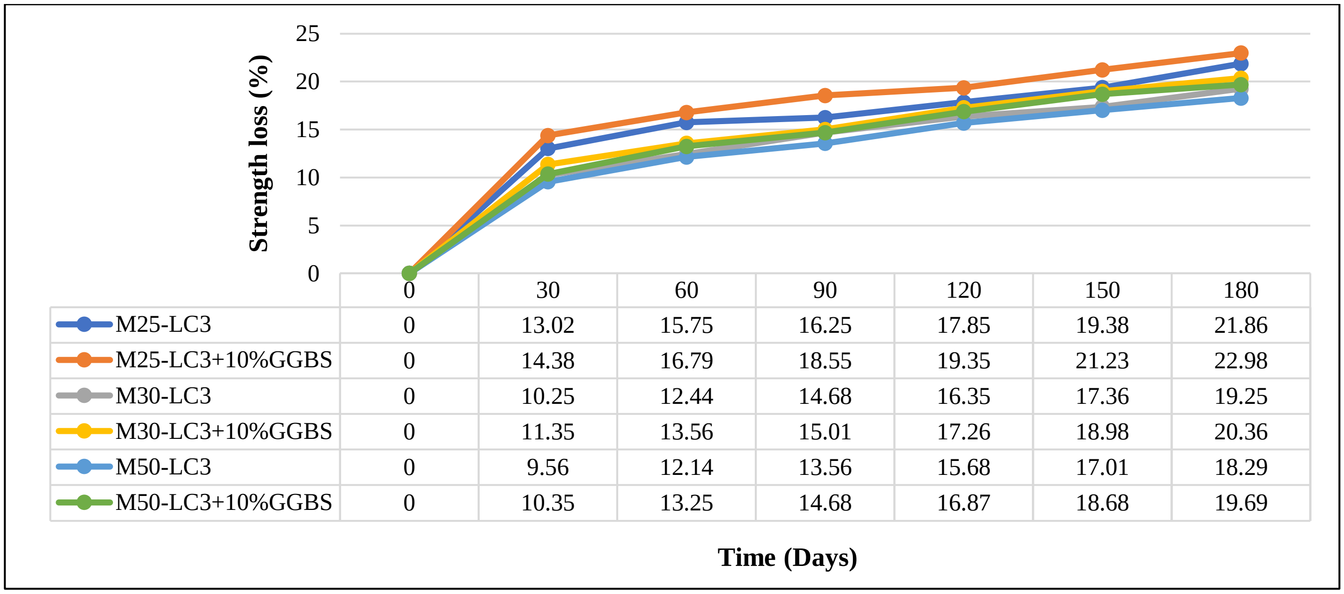

	0	30	60	90	120	150	180
M25-LC3	0	13.02	15.75	16.25	17.85	19.38	21.86
M25-LC3+10%GGBS	0	14.38	16.79	18.55	19.35	21.23	22.98
M30-LC3	0	10.25	12.44	14.68	16.35	17.36	19.25
M30-LC3+10%GGBS	0	11.35	13.56	15.01	17.26	18.98	20.36
M50-LC3	0	9.56	12.14	13.56	15.68	17.01	18.29
M50-LC3+10%GGBS	0	10.35	13.25	14.68	16.87	18.68	19.69

Fig. 9 Strength loss (%) of various LC3 concrete specimens after exposure to chloride solution

4.4. Water Absorption Test

The water absorption test results for various LC3 mixes, evaluated at 28 and 56 days, are presented in Figure 10. It was noted that the water absorption diminished as time increased. The water absorption rate of various LC3 mixes was in the range of 6.89%-7.87% at 28 days, where the water absorption rate of the LC3 mixes was found to be in the range of 6.40%-7.51%. This demonstrates that the water absorption rate declines as curing ages increase. The inclusion of LC3 significantly supports this trend through synergistic hydration reactions.

Limestone particles increase the packing density, while calcined clay contributes to the formation of additional alumina phases, and additional hydration products like carboaluminates further increase density and reduce permeability of hydrated phases [12]. This decline in water absorption rate from 28 to 56 days shows that the pozzolanic reaction in the LC3 system is effective in the gradual improvement of the concrete's resistance to water penetration. The inclusion of 10% of GGBS into the M25-LC3, M30-LC3, and M50-LC3 increases their water absorption rate to 7.87%, 7.59% and 6.89% from 7.51%, 7.12% and 6.56% at 28 days. Similarly, the inclusion of 10% of GGBS into the M25-LC3, M30-LC3, and M50-LC3 increases its water absorption rate to 7.51%, 6.99% and 6.58% from 7.32%, 6.79% and 6.40% at 56 days. As hydration progresses beyond 28 days, especially at 56 days, the GGBS-based LC3 concrete mix attains increased water resistance and low water absorption compared to the control LC3 concrete mix, resulting from the development of a denser microstructure. Moreover, GGBS exhibits pozzolanic and latent hydraulic properties, reacting with $Ca(OH)_2$ to form additional C-S-H gel, which improves the microstructure over time while minimizing voids and permeability within the matrix. Further, it was noted that low-strength concrete, such as M25 and M30 grade concrete, showed increased water absorption compared to the high compressive strength concrete (M50). The trends are consistent with previous findings, indicating that reduced porosity and enhanced particle distribution greatly diminish permeability. Generally, the inclusion of SCM heightens the water absorption rate. According to the replacement of 10% of GGBS into the LC3 cement, it shows a high water absorption rate. This finding was in line with Dixit et al. (2021), who demonstrated that inclusion of fly ash increases the water absorption rate of LC3 concrete [55]. Dixit et al. (2021) determined the water absorption rate of 7.2% for the fly ash-based LC3 concrete with 10% of fly ash at 28 days, whereas this study shows the water absorption rate of 6.89% for the GGBS-based LC3 concrete that contains 10% of GGBS at 28 days [55]. The lower water absorption (6.89%) in GGBS-based LC3 concrete, in contrast to fly ash-based LC3 (7.2%), results from GGBS's greater reactivity, denser microstructure, and enhanced pozzolanic-hydraulic synergy. These elements promote C-S-H formation, decrease porosity, and increase impermeability of the concrete.

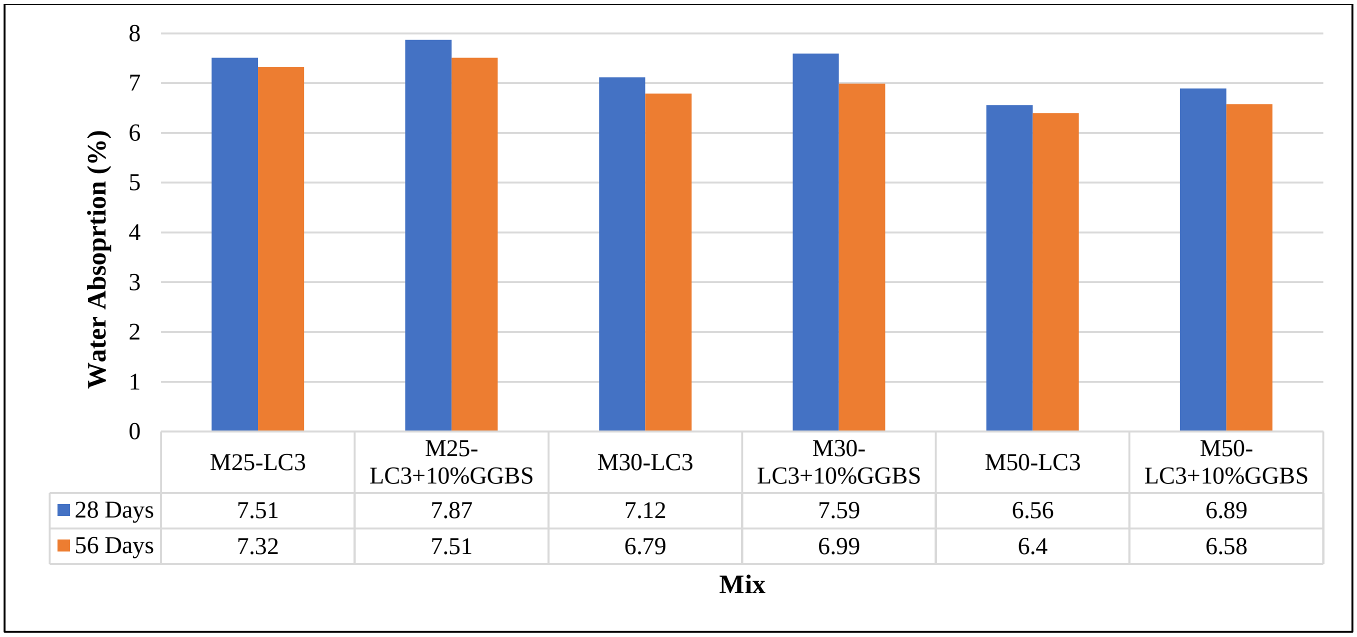

Fig. 10 Water Absorption (%) rate of various LC3 Concrete mixes

4.5. RCPT

ASTM C1202 provides a comprehensive categorization of the quality of concrete with reference to charge passed (ASTM C1202 2012) [56]. Figure 11 graphically displays the RCPT values of the various LC3 concrete at 28-days, 56-days, and 90-days. The findings demonstrate that LC3 cement concrete exhibits a low total charge passed at 28, 56, and 90-days, offering high resistance to chloride ion penetration. This similar finding was found to be in line with Sirangi & Prasad (2023), who reported that the LC3 concrete possesses superior chloride ion penetration resistance as compared to OPC and PPC concrete [5]. The enhanced reactivity potential of calcined clay present in the LC3 is the primary cause for the excellent chloride ion penetration resistance, which helps in forming a refined pore structure and a dense cement matrix.

This stops the flow of fluid medium into the concrete, thereby improving resistance to chloride penetration. As per ASTM C1202, the chloride resistance of LC3 concrete mixes falls under the "low" category of chloride ion penetration (ASTM C1202 2012). However, the inclusion of 10% GGBS into the LC3 concrete slightly increases the RCPT values (Charge passed). The inclusion of 10% of GGBS into the M25-LC3 increases its RCPT values by 37.45%, 32.86% and 44.67% at 28, 56, and 90 days. The inclusion of 10% of GGBS into the M30-LC3 increases its RCPT values by 27.89%, 22.94% and 14.24% at 28, 56, and 90 days. The inclusion of 10% of GGBS into the M50-LC3 increases its RCPT values by 8.51%, 7.74% and 8.26% at 28, 56, and 90 days. This increase in RCPT value of the LC3 concrete with the inclusion of 10% GGBS might be due to the physical, chemical, and microstructural changes caused by GGBS. In the LC3 system, the inclusion of GGBS contributes to the secondary hydration process, which can delay the microstructural densification during early stages of hydration, leading to increased porosity and hence increased susceptibility to chloride ion penetration.

Furthermore, GGBS interacts with $Ca(OH)_2$ to generate C-S-H, although this reaction might not completely enhance the pore structure during the early curing period. Additionally, GGBS minimally decreases the alumina content that can bind with chlorides in LC3, potentially resulting in increased chloride permeability, especially during the early curing phases. Although the inclusion of 10% of GGBS into the LC3 slightly increases the RCPT values, it still falls under the "low" category of chloride ion penetration. The superior resistance to chloride permeability was seen for the M50 grade concrete mix because of its high strength as well as dense matrix, since the M50 grade concrete was formulated with low w/c, which reduces the volume of capillary pores, resulting in a more compact microstructure that is less permeable to chloride ions.

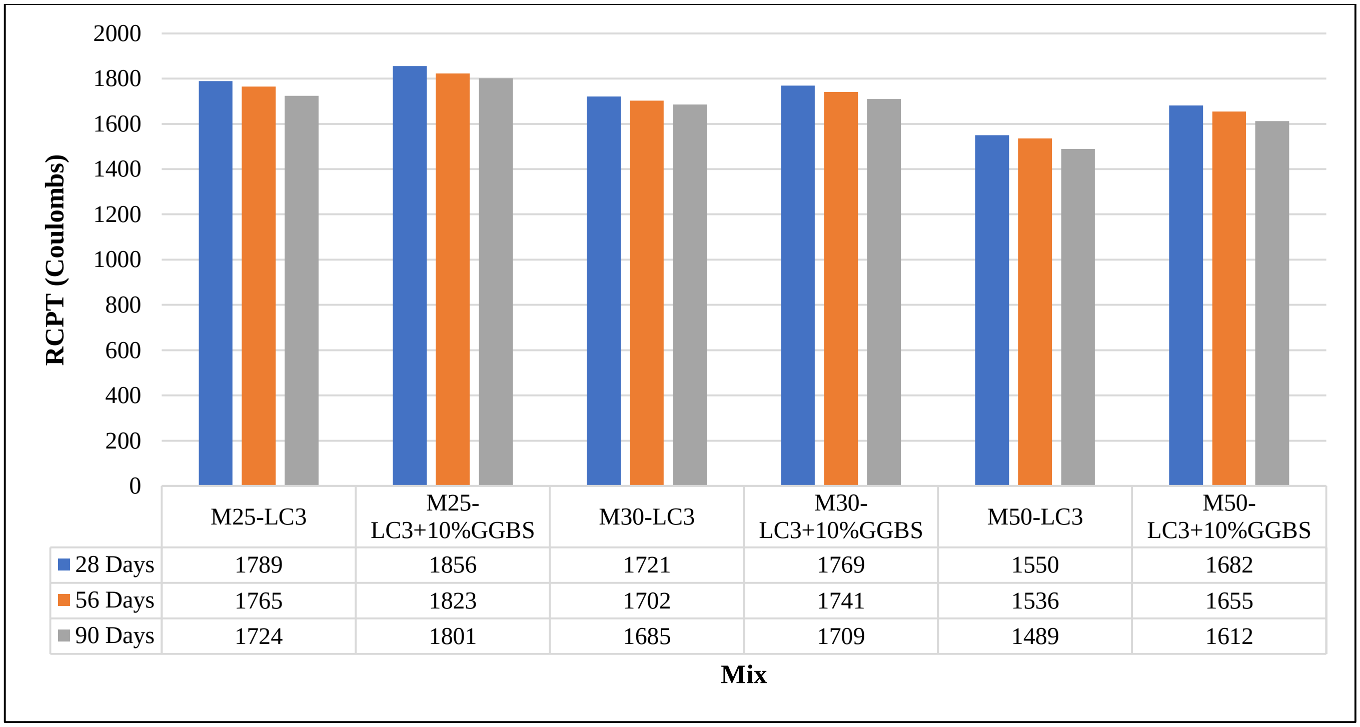

	M25-LC3	M25-LC3+10%GGBS	M30-LC3	M30-LC3+10%GGBS	M50-LC3	M50-LC3+10%GGBS
28 Days	1789	1856	1721	1769	1550	1682
56 Days	1765	1823	1702	1741	1536	1655
90 Days	1724	1801	1685	1709	1489	1612

Fig. 11 RCPT test results of various LC3 Concrete mixes

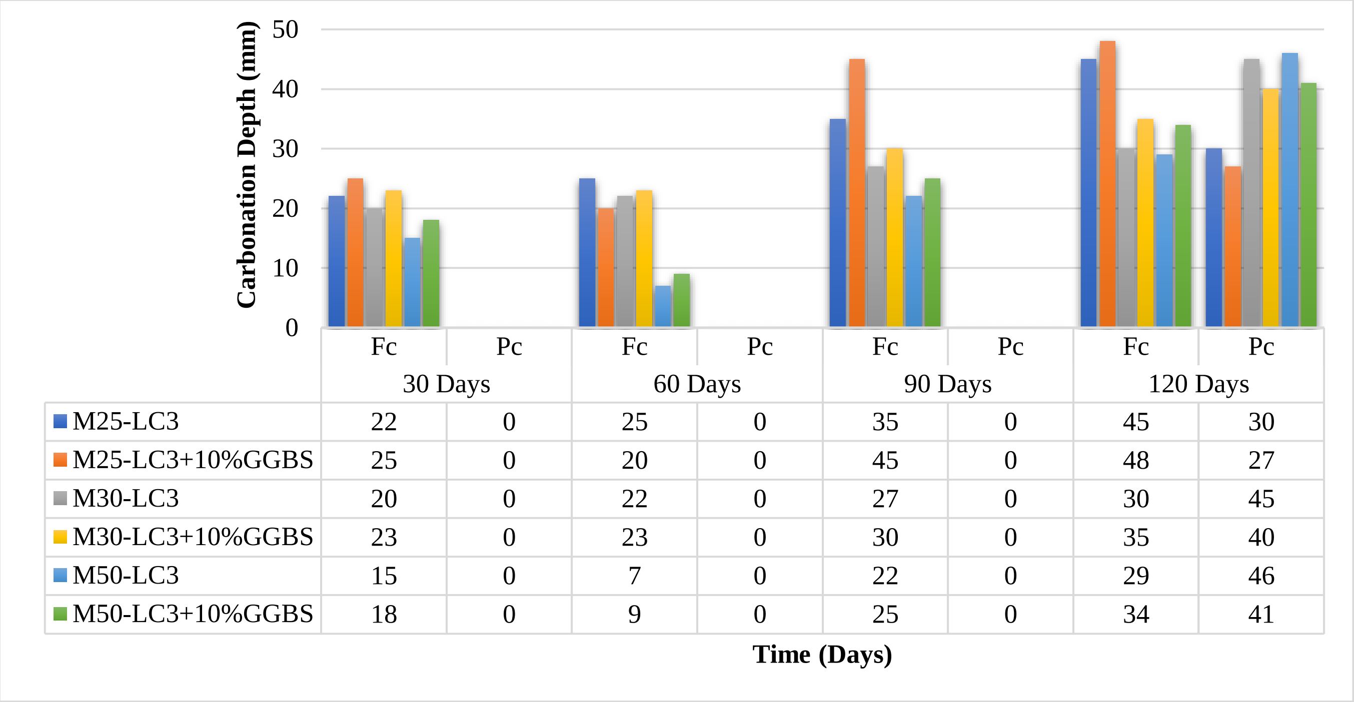

	30 Days		60 Days		90 Days		120 Days	
	Fc	Pc	Fc	Pc	Fc	Pc	Fc	Pc
M25-LC3	22	0	25	0	35	0	45	30
M25-LC3+10%GGBS	25	0	20	0	45	0	48	27
M30-LC3	20	0	22	0	27	0	30	45
M30-LC3+10%GGBS	23	0	23	0	30	0	35	40
M50-LC3	15	0	7	0	22	0	29	46
M50-LC3+10%GGBS	18	0	9	0	25	0	34	41

Fig. 12 Carbonation depth at various days of accelerated curing

Pc: Partial carbonation; Fc: Full carbonation

4.6. Carbonation Studies

Carbonation depth is one of the parameters to measure the durability property of concrete, as it influences the pH level within the concrete as a result of the interaction of CO_2 and $Ca(OH)_2$, which may cause reinforcement corrosion. The carbonation depths of the LC3 concrete specimen over 30, 60, 90, and 120 days are shown in Figure 12.

The pinkish color changes of specimens that were exposed to the accelerated carbonation were observed at intervals of 30 days up to 120 days, as illustrated in Figures 13-18.

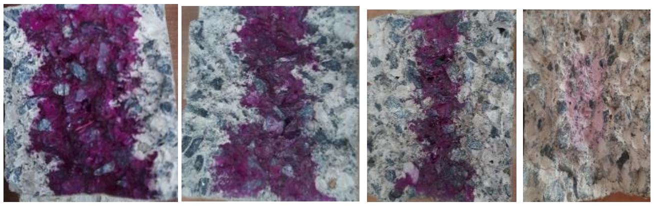
(a) 30-days (b) 60-days (c) 90-days (d) 120-days

Fig. 13 Pink color range of M25-LC3 samples

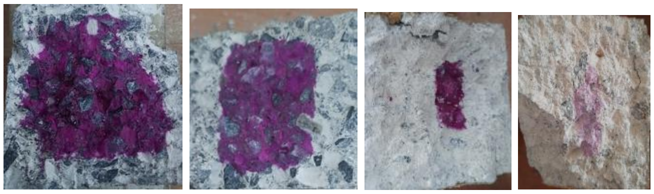
(a) 30-days (b) 60-days (c) 90-days (d) 120-days

Fig. 14 Pink color range of M25-LC3+10%GGBS samples

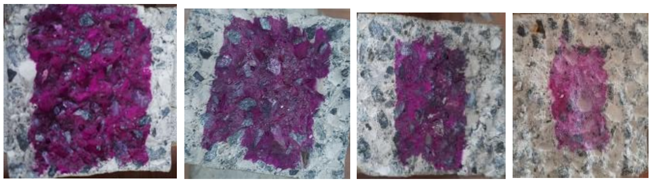
(a) 30-days (b) 60-days (c) 90-days (d) 120-days

Fig. 15 Pink color range of M30-LC3 samples

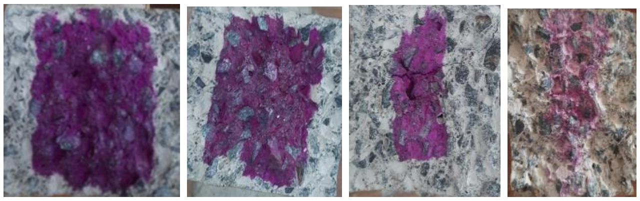
(a) 30-days (b) 60-days (c) 90-days (d) 120-days

Fig. 16 Pink color range of M30-LC3+10%GGBS samples

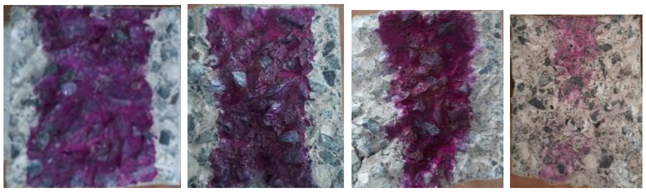
(a) 30-days (b) 60-days (c) 90-days (d) 120-days

Fig. 17 Pink color range of M50-LC3 samples

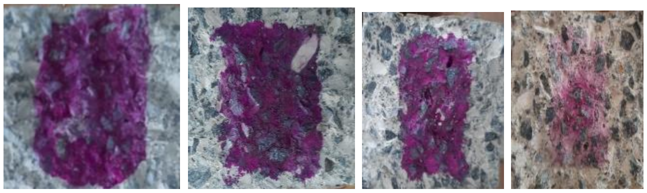
(a) 30-days (b) 60-days (c) 90-days (d) 120-days

Fig. 18 Pink color range of M50-LC3+10%GGBS sample

Existing studies reported that increased carbonation depth in concrete utilizing LC3 [6, 7]. At 30 and 60 days of testing, all the mix shows the Full Carbonation (Fc) without the Partial Carbonation (Pc). It was observed that the LC3 mixes contain 10% GGBS, which presents slightly higher carbonation depth than the respective control mixes. For example, the carbonation depth of M25-LC3+10% GGBS was about 25 mm, and M25-LC3 was 22mm at 30 days. The M25-LC3 mixture exhibits the highest carbonation depth, with the purple area gradually decreasing from 30 to 120 days, as illustrated in Figure 13. The M30-LC3 and M30-LC3 have slightly less carbonation depth than the M25-LC3; this mix also exhibits considerable carbonation, with a significant decrease in the purple area over time, as illustrated in Figures 15 and 17. However, the carbonation rises significantly by 120 days. In comparison to its control (M25-LC3), the M25-LC3+10%GGBS mix shows a notably lesser carbonation depth on all days. The purple region remains more prominent, even at 90 and 120 days, as shown in Figure 14.

The M30-LC3+10%GGBS demonstrates better carbonation resistance than M30-LC3. The purple coloration remains larger during the testing phase, as shown in Figure 16, suggesting reduced carbonation depth. The M50-LC3+10%GGBS blend shows the least carbonation depth, maintaining considerable purple coloration even after 120 days, showcasing excellent carbonation resistance as illustrated in Figure 18. The M30-LC3+10% GGBS and M50-LC3+10% GGBS achieved a reduction in depth of 23 mm and 18 mm, respectively, in comparison to 20 mm and 15 mm of their control mixes. This results from delayed pozzolanic reactions of GGBS, which causes a porous microstructure that allows deeper carbonation penetration of lime [23, 58]. At 90 days, significant differences in carbonation resistance were observed. GGBS-modified mixes such as M25-LC3+10% GGBS mixes show a carbonation depth of 45mm, whereas M25-LC3 shows a carbonation depth of 35mm. These same trends have been observed for M30 and M50 mixes, with the GGBS-modified mix showing higher carbonation depth. This is due to the presence of additional alumina phases introduced from GGBS, which potentially lead to less dense C-S-H gel formation and enhanced formation of calcium carbonate [12, 16].

Scrivener et al. (2018a) noted that LC3 systems exhibit reduced capability to combine with CO2 because of less availability of calcium free to react, since calcium is utilized in pozzolanic reaction involving SCMS such as GGBS, leading to a higher observed carbonation depth. The effects of GGBS were more pronounced at 120 days in terms of Partial Carbonation (Pc), especially for the higher-grade mixes M30 and M50. For example, an M30-LC3+10% GGBS had a partial carbonation depth of 40 mm, and that of the control mix was 45 mm. Greater depths of full carbonation were also observed in GGBS-modified mixes, including 48 mm for M25-LC3+10% GGBS compared to 45 mm for M25-LC3, highlighting the prolonged reactivity of GGBS in pore refinement. These findings show a clear interaction between LC3 and GGBS, where the addition of GGBS reduces the carbonation resistance due to delayed hydration but begins to densify the microstructure over time.

4.7. Environmental and Economic Impacts

The environmental impact of LC3-GGBS concrete was examined in terms of Embodied Carbon (EC) and Embodied Energy (EE) using "Inventory Carbon and Energy (ICE) Database v3.0" along with cost estimation to assess the economic impacts. Table 6 provides the EE, EC, and material cost of LC3 and LC3-GGBS concrete. Partial replacement of LC3 cement concrete by 10% GGBS reduces the EC, EE, and material cost by 20.16%-20.53%, 18.89%-21.07%, and 4.07%-4.71% respectively, with respect to various grades of concrete (M25, M30, and M50). The findings indicate that the lower energy intensity of GGBS significantly contributes to the observed carbon reduction.

Table 6. EC, EE, and material cost

Mix	EC (kg CO_2e/m^3)	EE (MJ/m^3)	Material Cost (₹/m^3)
M25-LC3	322.8	1562	3388
M25-LC3 + 10% GGBS	256.5	1261	3248
M30-LC3	333.3	1609	3436
M30-LC3 + 10% GGBS	266.1	1305	3296
M50-LC3	352.7	1713	3545
M50-LC3 + 10% GGBS	281.3	1352	3378

5. Conclusion

This study examines the partial replacement of LC3 cement concrete by GGBS on its durability properties, while also revealing the challenges in early-age performance under various exposure conditions. The various conclusions as observed from the findings are as follows;

- The incorporation of 10% GGBS into the LC3 cement concrete slightly increases the weight loss in all the concrete mixes. The M25-LC3+10% GGBS mix shows the highest weight loss of 43.88%, 29.61% and 20.58% after 180 days of acid, sulphate, and chloride exposure.
- The incorporation of 10% GGBS into the LC3 cement concrete slightly increases the weight loss in all the concrete mixes. The M25-LC3+10% GGBS mix shows the highest weight loss of 44.01%, 32.77% and 22.98% after 180 days of acid, sulphate, and chloride exposure.
- The high compressive strength (M50 grade) concrete displayed superior durability properties compared to the low compressive strength concrete (M25 and M30) due to its dense microstructure and lower water-cement ratios, effectively limiting acid, sulphate, and chloride ion ingress.
- The incorporation of 10% GGBS into the LC3 cement concrete slightly heightens the water absorption rate. The incorporation of 10% GGBS into the LC3 cement concrete increases the water absorption rate to 7.87%, 7.59% and 6.89% for M25-LC3, M30-LC3, and M50-LC3 concrete mix, respectively. However, the water absorption decreased with higher strength grades and extended curing times, indicating improved microstructural properties.
- The GGBS-modified LC3 concrete mixes exhibited higher carbonation depth compared to control mixes. The pozzolanic reaction of GGBS improved the long-term densification of the matrix but decreased the presence of free lime, which is essential for neutralizing chloride ions and resisting carbonation. However, the high compressive strength concrete mixes (M50) exhibited the least carbonation depth, highlighting enhanced resistance attributed to lower porosity and improved particle packing.

The findings emphasize the importance of dense microstructures in enhancing concrete durability. The delayed pozzolanic reaction of GGBS plays a significant part in the formation of dense microstructures. In the study, the samples are allowed to cure for a maximum period of 28 days; thus, the complete hydration process does not take place, which results in a slight increase in loss of weight and strength during 180 days exposure period. Therefore, future studies should use the samples that have been cured for a longer curing period to achieve complete pozzolanic reaction. This might have a positive effect on using GGBS in the LCE concrete. Furthermore, future studies should focus more on long-term durability investigations to determine their durability performance over an extended service period.

Acknowledgement

We extend our sincere thanks to the "Centre for Advanced Concrete Research – Civil (CACR-Civil), SRM Institute of Science and Technology, Kattankulathur" for their support with Equationipment in carrying out the research.

Author Contribution

K V: Methodology, conceptualization, writing-original draft; P.R.K- Resources, supervision, validation, writing-review and editing.

References

[1] Sajjad Ali, Salar Ahmad, and Ikram Ullah, "Utilization of Waste Marble Dust as Cement and Sand Replacement in Concrete," *Discover Civil Engineering*, vol. 1, pp. 1-11, 2024. [CrossRef] [Google Scholar] [Publisher Link]

[2] Arun Singh Chahar, and Priyaranjan Pal, "Investigation on Binary, Ternary, and Quaternary Blended Cement Mortar Integrated with Mineral Additives," *Iranian Journal of Science and Technology, Transactions of Civil Engineering*, vol. 48, pp. 3407-3439, 2024. [CrossRef] [Google Scholar] [Publisher Link]

[3] Bedshruti Sen et al., "Comparative Assessment of Energy Performance, GHG Emission, and Environmental Performance of Exterior Wall Alternatives for the Buildings in an Educational Campus in Kolkata, India," *Discover Civil Engineering*, vol. 2, pp. 1-25, 2025. [CrossRef] [Google Scholar] [Publisher Link]

[4] Safa Nayır, Ümit Bahadır, and Vedat Toğan, "Investigation of Global Warming Potential of Concrete with Silica Fume and Blast Furnace Slag," *Iranian Journal of Science and Technology, Transactions of Civil Engineering*, vol. 48, pp. 1965-1975, 2024. [CrossRef] [Google Scholar] [Publisher Link]

[5] Baris Erdil et al., "Structural Performance of Masonry Buildings under Harsh Climate and Seismic Loads," *Iranian Journal of Science and Technology, Transactions of Civil Engineering*, vol. 46, pp. 4031-4049, 2022. [CrossRef] [Google Scholar] [Publisher Link]

[6] Barbara Lothenbach, Karen Scrivener, and R.D. Hooton, "Supplementary Cementitious Materials," *Cement and Concrete Research*, vol. 41, no. 12, pp. 1244-1256, 2011. [CrossRef] [Google Scholar] [Publisher Link]

[7] Karen Scrivener et al., "Impacting Factors and Properties of Limestone Calcined Clay Cements (LC3)," *Green Materials*, vol. 7, no. 1, pp. 3-14, 2018. [CrossRef] [Google Scholar] [Publisher Link]

[8] M. Murat, "Hydration Reaction and Hardening of Calcined Clays and Related Minerals. I. Preliminary Investigation on Metakaolinite," *Cement and Concrete Research*, vol. 13, no. 2, pp. 259-266, 1983. [CrossRef] [Google Scholar] [Publisher Link]

[9] M. Antoni et al., "Cement Substitution by a Combination of Metakaolin and Limestone," *Cement and Concrete Research*, vol. 42, no. 12, pp. 1579-1589, 2012. [CrossRef] [Google Scholar] [Publisher Link]

[10] J. Ston, A. Hilaire, and K. Scrivener, "Autogenous Shrinkage and Creep of Limestone and Calcined Clay Based Binders," *Proceedings of the 2nd International Conference on Calcined Clays for Sustainable Concrete*, pp. 447-454, 2017. [CrossRef] [Google Scholar] [Publisher Link]

[11] François Avet et al., "Development of a New Rapid, Relevant and Reliable (R3) Test Method to Evaluate the Pozzolanic Reactivity of Calcined Kaolinitic Clays," *Cement and Concrete Research*, vol. 85, pp. 1-11, 2016. [CrossRef] [Google Scholar] [Publisher Link]

[12] Adrian Alujas et al., "Pozzolanic Reactivity of Low Grade Kaolinitic Clays: Influence of Calcination Temperature and Impact of Calcination Products on OPC Hydration," *Applied Clay Science*, vol. 108, pp.94-101, 2015. [CrossRef] [Google Scholar] [Publisher Link]

[13] Ernesto Díaz et al., "Carbonation of Concrete with Low Carbon Cement LC3 Exposed to Different Environmental Conditions," *Proceedings of the 2nd International Conference on Calcined Clays for Sustainable Concrete*, pp. 141-146, 2017. [CrossRef] [Google Scholar] [Publisher Link]

[14] M.S.H. Khan, Q.D. Nguyen, and A. Castel, "Carbonation of Limestone Calcined Clay Cement Concrete," *Proceedings of the 2nd International Conference on Calcined Clays for Sustainable Concrete*, pp. 238-243, 2017. [CrossRef] [Google Scholar] [Publisher Link]

[15] F. Avet et al., "Development of a New Rapid, Relevant and Reliable (R3) Testing Method to Evaluate the Pozzolanic Reactivity of Calcined Clays," *Proceedings of the 1st International Conference on Calcined Clays for Sustainable Concrete*, pp. 539-544, 2015. [CrossRef] [Google Scholar] [Publisher Link]

[16] Rodrigo Fernandez Lopez, "*Calcined Clayey Soils as a Potential Replacement for Cement in Developing Countries*," Doctoral Thesis No. 4309, ECOLE Federal Polytechnic School of Lausanne, pp. 1-153, 2009. [Google Scholar] [Publisher Link]

[17] V.L. Bonavetti, V.F. Rahhal, and E.F Irassar, "Studies on the Carboaluminate Formation in Limestone Filler-Blended Cements," *Cement and Concrete Research*, vol. 31, no. 6, pp. 853-859, 2001. [CrossRef] [Google Scholar] [Publisher Link]

[18] V. Renuka, Sarella Venkateswara Rao, and Tezeswi Tadepalli, "State-of-the-art Review on Limestone Calcined Clay Cement (LC3) and its Recent Advances," *Iranian Journal of Science and Technology, Transactions of Civil Engineering*, pp. 1-30, 2025. [CrossRef] [Google Scholar] [Publisher Link]

[19] Yuvaraj Dhandapani et al., "Mechanical Properties and Durability Performance of Concretes with Limestone Calcined Clay Cement (LC3)," *Cement and Concrete Research*, vol. 107, pp. 136-151, 2018. [CrossRef] [Google Scholar] [Publisher Link]

[20] Yuvaraj Dhandapani, and Manu Santhanam, "Assessment of Pore Structure Evolution in the Limestone Calcined Clay Cementitious System and its Implications for Performance," *Cement and Concrete Composites*, vol. 84, pp. 36-47, 2017. [CrossRef] [Google Scholar] [Publisher Link]

[21] Sreejith Krishnan, C. Arun Emmanuel, and Shashank Bishnoi, "Hydration and Phase Assemblage of Ternary Cements with Calcined Clay and Limestone," *Construction and Building Materials*, vol. 222, pp. 64-72, 2019. [CrossRef] [Google Scholar] [Publisher Link]

[22] S.H. Mohammad Khan, Quang Dieu Nguyen, and Arnaud Castel, "Performance of Limestone Calcined Clay Blended Cement-based Concrete Against Carbonation," *Advances in Cement Research*, vol. 32, no. 11, pp. 481-491, 2020. [CrossRef] [Google Scholar] [Publisher Link]

[23] M. Shiva Kumar, and Thirumalini Selvaraj, "Ancient Organic Lime Plaster Production Technology and its Properties among Mayan, Egyptian, Persian and Asian Civilizations," *Asian Journal of Civil Engineering*, vol. 24, pp. 2709-2718, 2023. [CrossRef] [Google Scholar] [Publisher Link]

[24] Kiran Ram et al., "Influence of Low- to Medium-Kaolinite Clay on the Durability of Limestone Calcined Clay Cement (LC3) Concrete," *Materials*, vol. 16, no. 1, pp. 1-18, 2022. [CrossRef] [Google Scholar] [Publisher Link]

[25] UN Environment et al., "Eco-Efficient Cements: Potential Economically Viable Solutions for a Low-CO_2 Cement-Based Materials Industry," *Cement and Concrete Research*, vol. 114, pp. 2-26, 2018. [CrossRef] [Google Scholar] [Publisher Link]

[26] Quang Dieu Nguyen et al., "Autogenous and Total Shrinkage of Limestone Calcined Clay Cement (LC^3) Concretes," *Construction and Building Materials*, vol. 314, 2022. [CrossRef] [Google Scholar] [Publisher Link]

[27] Marwan Abdulqader et al., "Physicochemical Properties of Limestone Calcined Clay Cement (LC3) Concrete made using Saudi Clays," *Journal of Materials Research and Technology*, vol. 25, pp. 2769-2783, 2023. [CrossRef] [Google Scholar] [Publisher Link]

[28] Carlos Eduardo Tino Balestra et al., "Carbonation of Concretes Containing LCÂ³ Cements with Different Supplementary Materials," *Semina: Ciências Exatas e Tecnológicas*, vol. 43, no. 2, pp. 161-170, 2022. [CrossRef] [Google Scholar] [Publisher Link]

[29] Y.D. Cárdenas, E.D. Caballero, and J.F. Martirena-Hernandez, "Evaluation of Carbonation in Specimens Made with LC3 Low Carbon Cement," *Proceedings of the International Conference of Sustainable Production and Use of Cement and Concrete: ICSPCC 2019*, Villa Clara, Cuba, pp. 307-317, 2019. [CrossRef] [Google Scholar] [Publisher Link]

[30] Yudiesky Cancio Díaz et al., "Limestone Calcined Clay Cement as a Low-Carbon Solution to Meet Expanding Cement Demand in Emerging Economies," *Development Engineering*, vol. 2, pp. 82-91, 2017. [CrossRef] [Google Scholar] [Publisher Link]

[31] Dandan Kong et al., "Enhancing Carbonation Resistance of Low-Activity Coal Gangue-Based LC^3 Cementitious Materials with $Ca(OH)_2$ and Gypsum Additivess," *Journal of Building Engineering*, vol. 98, 2024. [CrossRef] [Google Scholar] [Publisher Link]

[32] Musaad Zaheer Nazir Khan et al., "Mechanical Properties of Ambient Cured High Strength Hybrid Steel and Synthetic Fibers Reinforced Geopolymer Composites," *Cement and Concrete Composites*, vol. 85, pp. 133-152, 2018. [CrossRef] [Google Scholar] [Publisher Link]

[33] Vineet Shah, and Shashank Bishnoi, "Carbonation Resistance of Cements Containing Supplementary Cementitious Materials and its Relation to Various Parameters of Concrete," *Construction and Building Materials*, vol. 178, pp. 219-232, 2018. [CrossRef] [Google Scholar] [Publisher Link]

[34] Yaocheng Wang et al., "Corrosion Mechanism of Reinforcement in LC3 Cement Pastes under Coupled Carbonation and Chloride Attack," *Cement and Concrete Composites*, vol. 140, 2023. [CrossRef] [Google Scholar] [Publisher Link]

[35] Carlos Eduardo Tino Balestra et al., "Contribution to Low-Carbon Cement Studies: Effects of Silica Fume, Fly Ash, Sugarcane Bagasse Ash and Acai Stone Ash Incorporation in Quaternary Blended Limestone-Calcined Clay Cement Concretes," *Environmental Development*, vol. 45, 2023. [CrossRef] [Google Scholar] [Publisher Link]

[36] Lei Wang et al., "Effects of Fly Ash Dosage on Shrinkage, Crack Resistance and Fractal Characteristics of Face Slab Concrete," *Fractal and Fractional*, vol. 6, no. 6, pp. 1-20, 2022. [CrossRef] [Google Scholar] [Publisher Link]

[37] Jofre Mañosa et al., "Research Evolution of Limestone Calcined Clay Cement (LC^3), A Promising Low-Carbon Binder – A Comprehensive Overview," *Heliyon*, vol. 10, no. 3, pp. 1-14, 2024. [CrossRef] [Google Scholar] [Publisher Link]

[38] Indian Standard: 383-2016, "*Coarse and Fine Aggregate for Concrete - Specification*," Bureau of Indian Standard, New Delhi, pp. 1-21, 2016. [Google Scholar] [Publisher Link]

[39] IS 2386-3 (1963): "*Methods of Test for Aggregates for Concrete*," Part 3: Specific Gravity, Density, Voids, Absorption and Bulking, Bureau of Indian Standard, New Delhi, pp. 1-22, 1963. [Google Scholar] [Publisher Link]

[40] Indian Standard: 10262-2019, "*Concrete Mix Proportioning -Guideline*," Bureau of Indian Standard, New Delhi, pp. 1-44, 2019. [Google Scholar]

[41] Indian Standard 516: Part 1: Sec 1: 2021, "*Hardened Concrete Methods of Test*," Part 1 Testing of Strength of Hardened Concrete Section 1 Compressive, Flexucal and Split Tensile Strength (First Revision), Bureau of Indian Standard, New Delhi, 2021. [Google Scholar] [Publisher Link]

[42] *ASTM C267 Chemical Resistance of Mortars, Grouts, and Monolithic Surfacings and Polymer Concretes*, American Society for Testing and Materials, pp. 1-6, 2001. [Publisher Link]

[43] *ASTM C267-97 - Standard Test Methods for Chemical Resistance of Mortars, Grouts, and Monolithic Surfacings and Polymer Concretes*, American Society for Testing and Materials, pp. 1-3, 1997. [Publisher Link]

[44] K. Kawai, S. Yamaji, and T. Shinmi, "Concrete Deterioration Caused by Sulfuric Acid Attack," *Durability of Building Materials*, pp. 5-9, 2005. [Google Scholar]

[45] Onesmus Mulwa Munyao et al., "Study on the Effect of Thiobacillus Intermedius Bacteria on the Physico-Mechanical Properties of Mortars of Ordinary Portland Cement," *Heliyon*, vol. 6, no. 1, pp. 1-8, 2020. [CrossRef] [Google Scholar] [Publisher Link]

[46] Bing Tian, and Menashi D. Cohen, "Does Gypsum Formation during Sulfate Attack on Concrete Lead to Expansion?," *Cement and Concrete Research*, vol. 30, no. 1, pp. 117-123, 2000. [CrossRef] [Google Scholar] [Publisher Link]

[47] J. Joseph Mwiti Marangu, "Effects of Sulfuric Acid Attack on Hydrated Calcined Clay–Limestone Cement Mortars," *Journal of Sustainable Cement-Based Materials*, vol. 10, no. 5, pp. 257-271, 2021. [CrossRef] [Google Scholar] [Publisher Link]

[48] Siva Shanmukha Anjaneya Babu Padavala et al., "Bond Strength of Fly Ash and Silica Fume Blended Concrete Mixes," *Asian Journal of Civil Engineering*, vol. 25, pp. 895-909, 2024. [CrossRef] [Google Scholar] [Publisher Link]

[49] Vera Correia et al., "Effect of the Addition of GGBS on the Frost Scaling and Chloride Migration Resistance of Concrete," *Applied Sciences*, vol. 10, no. 11, pp. 1-21, 2020. [CrossRef] [Google Scholar] [Publisher Link]

[50] Zhenguo Shi et al., "Sulfate Resistance of Calcined Clay – Limestone – Portland Cements," *Cement and Concrete Research*, vol. 116, pp. 238-251, 2019. [CrossRef] [Google Scholar] [Publisher Link]

[51] Paweł Łukowski, and Ali Salih, "Durability of Mortars Containing Ground Granulated Blast-furnace Slag in Acid and Sulphate Environment," *Procedia Engineering*, vol. 108, pp. 47-54, 2015. [CrossRef] [Google Scholar] [Publisher Link]

[52] P. Mehta, and Paulo J.M. Monteiro, *Concrete Microstructure, Properties, and Materials*, McGraw-Hill Education, pp. 1-659, 2006. [Google Scholar] [Publisher Link]

[53] Adam M. Neville, *Properties of Concrete*, Pearson, pp. 1-846, 2011. [Google Scholar] [Publisher Link]

[54] H.F.W. Taylor, *Cement Chemistry*, Emerald Publishing Limited, pp. 1-459, 1997. [CrossRef] [Google Scholar] [Publisher Link]

[55] Anjaneya Dixit, Hongjian Du, and Sze Dai Pang, "Performance of Mortar Incorporating Calcined Marine Clays with Varying Kaolinite Content," *Journal of Cleaner Production*, vol. 282, pp. 1-30, 2021. [CrossRef] [Google Scholar] [Publisher Link]

[56] ASTM C1202, *Standard Test Method for Electrical Indication of Concrete's Ability to Resist Chloride Ion Penetration*, pp. 1-8, 2012. [Google Scholar] [Publisher Link]

[57] Bhavani Sirangi, and M.L.V. Prasad, "A Low Carbon Cement (LC3) as a Sustainable Material in High Strength Concrete: Green Concrete," *Construction Materials*, vol. 73, no. 352, pp. 1-12, 2023. [CrossRef] [Google Scholar] [Publisher Link]

[58] Yuvaraj Dhandapani, and Manu Santhanam, "Investigation on the Microstructure-Related Characteristics to Elucidate Performance of Composite Cement with Limestone-Calcined Clay Combination," *Cement and Concrete Research*, vol. 129, 2020. [CrossRef] [Google Scholar] [Publisher Link]